

Connecting single-molecule and superresolution microscopies to cell biology through theoretical modeling

Jian Liu^{1,*} and Taekjip Ha^{2,3,*}

¹Department of Cell Biology, Center for Cell Dynamics, School of Medicine, Johns Hopkins University, Baltimore, Maryland; ²Howard Hughes Medical Institute and Program in Cellular and Molecular Medicine, Boston Children's Hospital, Boston, Massachusetts; and ³Department of Pediatrics, Harvard Medical School, Boston, Massachusetts

ABSTRACT Recent developments of single-molecule and superresolution microscopies reveal novel spatial-temporal features of various cellular processes with unprecedented details, and greatly facilitate the development of theoretical models. In this review, we synthesize our view of how to meaningfully integrate these experimental approaches with theoretical modeling to obtain deeper understanding of the physical mechanisms of cell biology.

SIGNIFICANCE We give a few examples drawn from recent cell biological studies utilizing single-molecule and superresolution imaging tools that benefit from theoretical modeling, not only to describe the phenomenon but also to stimulate further experimentation through testable predictions.

INTRODUCTION

Cell biology interrogates the basic unit of life. Currently, predictive theoretical models lack experimental data due to the need to integrate across scales. Cellular processes typically emerge through the collective behaviors of tens to hundreds of different kinds of molecular players at a mesoscale, i.e., at the length scale of hundreds of nanometers to microns and at the timescale of seconds to minutes. From a theory standpoint, the framework at the mesoscale is underdeveloped compared with microscopic and macroscopic models available. Theory on the mesoscale cell biology may build upon the average behaviors of key components by integrating out their fast degrees of freedom, since the conformational fluctuations of a single protein are not expected to affect the collective behaviors at the long timescale. But there are at least two unsettled problems. First, it is not well understood exactly to what extent the fast degrees of freedom can be averaged out in depicting the cellular behaviors. Biological systems are proposed to

operate near a critical point in the control parameter space (1,2), which enables the rapid adaption to environmental changes. A feature of the criticality is that a minuscule change may be amplified to greatly perturb the entire system. Consequently, there may not be a clear separation in the molecules' degrees of freedoms from the mesoscale phenomenon. Second, for most cellular events, we are still in the process of identifying key players.

Cell biology experiments, however, have their own difficulty. The foremost hurdle has been the insufficient resolutions of live-cell imaging—it is difficult to achieve the resolution beyond diffraction limit of light (~ 200 nm). And yet, many of the essential/interesting events of cellular processes occur at scales of tens to hundreds of nanometers. The recently developed single-molecule and superresolution imaging techniques can reveal novel spatial-temporal features that put stronger constraints on the possible physical mechanisms and greatly facilitate the development of theoretical models.

In this review, we summarize our view of how single-molecule and superresolution microscopies can meaningfully engage with theoretical models to obtain a deeper mechanistic understanding of cellular processes. We illustrate our points through a few examples of our recent work. Although spanning over different topics, we hope

Submitted August 17, 2024, and accepted for publication November 22, 2024.

*Correspondence: jiu187@jhmi.edu or taekjip.ha@childrens.harvard.edu

Editor: Christy Landes.

<https://doi.org/10.1016/j.bpj.2024.11.3308>

© 2024 Biophysical Society. Published by Elsevier Inc.

All rights are reserved, including those for text and data mining, AI training, and similar technologies.



that these examples may convey a coherent style of approaches. For each topic below, we do not aim to have a comprehensive review. Rather, we endeavor to provide the necessary background with both the essential details and a bird's eye view of the cell biological process in question, which sets the proper stage for the readers to appreciate how to formulate the "right" questions, why experiments and theoretical models are designed in a specific manner, and what impactful conclusions and future directions can be uniquely drawn through the chosen approach?

FOCAL ADHESION-MEDIATED CELL PROTRUSION AND RETRACTION

Focal adhesion (FA) is a transmembrane protein assembly through which the cell exerts contractile forces to adhere to and migrate on the extracellular matrix (ECM) (3,4). During adhesion and migration, the cell constantly protrudes and retracts the membrane of its edge to explore the surroundings. Integrating the information from FA and cell edge protrusion/retraction helps the cell determine its next move, either staying put or migrating to chase the environmental cues. Episodes of adhesion, protrusion, retraction, and migration constitute the fundamental events of cell motility, important for many physiological functions (e.g., vascular maintenance (5) and cancer metastasis (6)). However, for a major adhesion and force-transmission apparatus, FA is surprisingly labile (3,4). It assembles and disassembles *de novo*, and dynamically adapts its ECM-contacting domain composition, size, and shape to the mechanical changes of the cell and its environment. While this plastic modality of FA is reported to underlie a cellular strategy of efficient mechanosensing of the ECM stiffness (7,8), it is unclear how such a labile FA coordinates with cell edge protrusion and retraction in the decision making of cell motility. Given that there are more than 100 different types of proteins involved in FA dynamics and cell motility (9), how could we even think about this complex process in a rational and quantitative manner?

Two of our recent works addressed this question under different cellular contexts, and collectively revealed an underappreciated but overarching theme (10,11) of a tripartite feedback system between FA life cycle, actin cytoskeleton dynamics, and local cell edge protrusion/retraction. Before delving into some details of how the organic integration of theory with single-molecule and superresolution microscopies leads to the key findings, let us briefly introduce the essential elements of FA, cell motility, and contractility.

As a cell adheres onto the ECM, the membrane tension regulates cell spreading through its impact on cell membrane edge dynamics (3,4). Here, membrane tension *in vivo* is the sum of the intrinsic membrane tension of the lipid bilayer due to the hydrophobicity between the lipid-water interface and the contractility (also known as cortical ten-

sion) arising from cytoskeleton-membrane adhesion; it "holds" up the cell shape against the intracellular stress from osmotic pressure and protrusive forces and is predominantly determined by cortical tension (12,13). Meanwhile, branched actin network polymerizes against the cell membrane, resulting in a combination of a forward protrusion of the cell leading edge and the retrograde actin flux, which is a backward flow of the branched actin network relative to the ECM (3,4). Concurrently, the cell seeds many nascent focal complexes near its leading edge, many of which disassemble rapidly. The surviving focal complexes mature to become FAs (3,4) by growing centripetally toward the interior of the cell, propelled by the retrograde actin flux and by engaging with the stress fiber (SF) and transmitting the associated actomyosin contractile forces onto the ECM. FA displays remarkable mechanochemical features across three different levels. At the molecular level, a transmembrane protein integrin links the ECM to the actin cytoskeleton via adaptor proteins (e.g., talin and vinculin), constituting the main element of FA force-transmission machinery. At the single-FA level, a mature FA is a micron-sized structure consisting of many force-transmission complexes that display distinctive FA-localized activities (7,8,14,15), linking FA maturation to mechanosensing. Beyond the single-FA level, directed cell motility must coordinate the cell edge protrusion/retraction with the cell body movement driven by the FA-mediated contractile forces.

Everything should be made as simple as possible, but not simpler.

—Albert Einstein

We now dissect the logic behind constructing the model of interaction between FA and cell edge (7,10,11). With the aim of building the simplest physical model with biological relevance, we envisioned three key model ingredients (Fig. 1). First, an FA mechanically interacts with the local cell edge via the branching actin network in between (Fig. 1 A). The FA-bound adaptor proteins impede the local actin flow by "grabbing" the actin cytoskeleton (16,17). This FA-actin interaction anchors the polymerization of branching actin network, protruding the local cell edge against the membrane tension (18). This notion is consistent with the observation that disrupting FA-actin flux engagement abolishes cell protrusion (19). Second, the anchoring effect of FA is not constant because the mechanical engagement with the actin retrograde flux and SF modulates the biochemical reactions (20–23) that underlie FA centripetal growth and maturation (Fig. 1 B). Third, cell edge protrusion and retraction greatly impact the actin retrograde flow due to the mass conservation of actin polymerization: i.e., the rate of actin retrograde flux plus the rates of cell edge protrusion should be equal to the polymerization rate of the branching actin network. Taken together, the model depicts the tripartite feedback between the FA

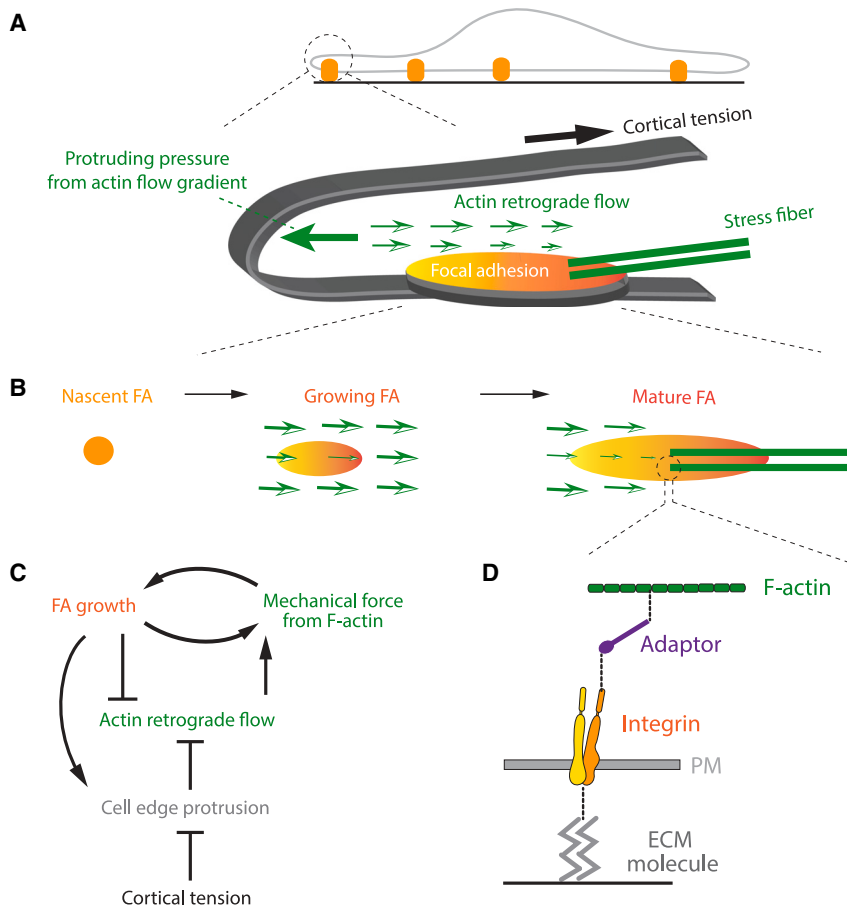


FIGURE 1 Schematics describing the multiscale tripartite feedback between focal adhesion (FA) growth, actin retrograde flow, and cell edge protrusion/retraction. (A) Overall model scheme of FA-cell edge interactions mediated by actin retrograde flow. It is a side view illustration of the major mechanical elements. (B) Schematized FA growth from nascent state, growing state to maturation that couple to actin retrograde flow and stress fiber contractility. (C) Diagrammatic model scheme of tripartite feedback between FA, actin retrograde flow, and cell edge protrusion. The FA growth feeds back with the impinging mechanical force from F-actin, including stress fiber contractility and the mechanical engagement with actin retrograde flow. FA provides the anchorage effect that effectively protrudes the cell edge, which is counteracted by the membrane tension that holds back the cell edge. Therefore, the protrusion of cell edge “let it go” the polymerization of branching actin network, decreasing the actin retrograde flow and hence closing the tripartite feedback loop. (D) Zoom-in view of the multiscale model. The model describes the three-layered structure of force-transmission element in FA and captures the observed catch bond and slip bond behaviors. The thick dashed line represents the chemical bond connecting the neighboring molecules in the layered structure. Note, for illustration purposes, individual components the schematics in (A), (B), and (D) do not reflect the true relative sizes. In reality, a nascent FA is approximately a few hundreds of nanometers in diameter; a mature FA is approximately several microns long and approximately one micron wide; integrins, adaptor proteins, and actin subunit are large molecules that range from several to tens of nanometers in their longest linear dimension.

dynamics, local actin flux, and cell edge protrusion/retraction (Fig. 1 C).

When we solved the mathematically formulated model self-consistently, the cell edge is protruded by the internal pressure arising from the spatial variation of actin retrograde flux and is retracted by the membrane tension. Further, in contrast to other models that abstract the FA as a geometric point without internal spatial features (24), our model depicts how a nascent FA grows centripetally by the mechanical interactions with actin retrograde flux, matures into the SF-engaging FA, and transmits the associated traction forces onto the ECM (7). To capture the essence of FA plastic modality, we described FA as a three-layered structure (Fig. 1 D): ECM, integrin, and FA adaptor occupy their own layers (25); the bonding in between can be on and off, depending on the mechanical challenges by actin flow and SF; and, once the bonding is off, the corresponding participants (e.g., adaptor itself) can drift with the local actin flow and deposit downstream, underlying the FA centripetal growth (16). This mathematical framework provides three advantages (7). First, it not only meaningfully engages with experiments but allows us to look beyond the roles of individual molecular players and discern the collective behavior of functional modules on a system level. Conse-

quently, it quantitatively establishes the mechanistic origin of the force oscillations within an FA, where the FA traction peak apparently travels back and forth along the long axis of FA while oscillating in amplitude (7). Second, the model accurately describes the geometry of growing FA and the associated hydrodynamic profile of actin retrograde flow (16,17). Third, it provides quantitative and falsifiable predictions that perturb either FA or actin flow, or cell edge dynamics will impact the other two.

Rigorous experimental testing of the model, however, proved to be difficult. Particularly, it was challenging to specifically perturb the FA formation while simultaneously imaging FA, actin flux, and cell edge dynamics in a living cell.

Give us the tools, and we will finish the job.

—Winston Churchill

As a force-bearing element between ECM and actin, integrin is believed to undergo conformational activation modulated by ligand binding, tension, and intracellular signaling. To control the single-molecular forces that can be experienced by an integrin-ligand bond, we developed a tension gauge tether (TGT) (26,27), where an ECM ligand for integrin is immobilized on the surface through a DNA

tether. Because the tether ruptures if the tension applied by the cell through the integrin is larger than its tension tolerance, the TGT serves as an autonomous gauge to restrict the receptor-ligand tension. Using a range of tethers with tunable tension tolerance, one can quantify the tension required for signal activation by observing FA-based cell activities, which are usually much easier to detect than single-molecule events. Importantly, because each ligand is equipped with an individual tension gauge, the single-molecule force information can be performed at very high receptor or ligand density which would normally preclude single-molecule fluorescence imaging. Using the TGT, we showed that cells apply a universal peak tension of ~ 40 pN to single integrin-ligand bonds during initial adhesion. To better monitor the tension per integrin molecule within FA in real time, we further developed the quenched TGT (qTGT) (28). Here, the DNA tether is a zipper with the Cy3 fluorescence dye fused onto one half of the zipper and a quencher on the other half. Consequently, the fluorescence is quenched in an intact DNA tether but is restored when the DNA tether ruptures. Now using this qTGT in combination with total internal reflection fluorescence microscopy (TIRFM) and reflection interference contrast microscopy (RICM), we can simultaneously visualize in real time the tension on integrin, FA formation, and the topography of the ventral cell membrane, respectively. We are therefore ready to quantitatively dissect the physical mechanisms underlying FA-cell edge interactions.

Asking the right questions is as important as answering them.

—Benoit Mandelbrot

One example is the human airway smooth muscle (hASM) cells that retract in response to stimuli (e.g., histamine) to control the diameter of the lung airway; the deregulations of hASM retraction are believed to contribute to asthma. We found that 1) hASM cells could spread on surfaces with strong TGTs, 2) histamine stimulation invokes calcium influx that activates actomyosin contractility, and 3) after histamine, the initially spreading hASM cells eventually undergo cell shortening, likely through cell edge retraction, with a time delay that increases with TGT strength (10). These interesting observations help shape the right questions. Why does the cell spread only with strong TGT? And what hinders the hASM cell retraction as actomyosin contractility is heightened to pull back the cell edge?

Intuition is a very powerful thing, more powerful than intellect, in my opinion.

—Steve Jobs

Intuitively, perhaps the FAs are too strong to disassemble immediately after calcium influx, hence mechanically hindering the actin retrograde flux and the cell edge retraction.

To test whether this intuition makes physical sense, we first adapted our mathematical model with realistic parameters to capture the essence of our experiments in two ways (10): 1) once the tension per integrin molecule exceeds T_{tol} and the TGT rips off from the substrate, the turnover rate of integrin will increase drastically triggering the FA disassembly and 2) the calcium influx-mediated activation of actomyosin contractility increases both the membrane tension and the SF contractility. Our model calculations recapitulated the observed dependences of both the cell spreading and the retraction time delay on TGT strength (10). Actin retrograde flow impinges upon a nascent FA complex with a significant force, which ruptures weak TGTs. This causes the disassembly of the nascent FA complex; hence, without stable FA anchorage, the cell edge cannot protrude efficiently, preventing cell spreading. Conversely, with strong TGTs, the nascent FA complexes can withstand the force from the actin flow and grow into the mature FAs, supporting cell spreading. Subsequent stimulation with histamine activates the SF's actomyosin contractility, which strengthens the associated mature FA, which further increases the SF contractile force through positive feedback until it becomes large enough to rupture even the TGTs, triggering the FA disassembly. Therefore, the stronger a TGT is, the longer it takes for the associated FA to disassemble and for the cell edge to retract (10).

How do we further test the model experimentally? According to our model, the SF contractility increase should simultaneously strengthen the FA. We further reasoned that, if so, then the distance between the ventral cell membrane and the substrate should decrease concurrently with the FA strengthening, until FA disassembles upon qTGT rupture. Indeed, high-resolution live-cell imaging data measuring three different activities simultaneously support these predictions. Right before the FA disassembly and cell edge retraction induced by histamine, the FA strengthened (as seen via an FA marker, paxillin-GFP, signal increase detected in TIRFM) and the cell adhered to the substrate more tightly (as seen by RICM). Importantly, the two events reached their peaks when the local force greatly increased (as seen via qTGT signals). These quantitative model-experiment agreements led us to conclude that SF contractility-mediated FA development needs to be properly coordinated with membrane tension for a timely airway contraction/dilation upon stimuli.

In any field find the strangest thing and then explore it.

—John Archibald Wheeler

Thus far, we could link cell edge retraction with FA activities. Can we also establish a mechanical connection between cell edge protrusion and FA activities? When exploring cell migration in a high-viscosity environment, the laboratory of Yun Chen discovered an unusual phenomenon (11). When subjected to a highly viscous solution,

many different cell types sped up their migration with extensive spreading accompanied by rapid suppression of membrane ruffling on the upper side of the adherent cell (termed “dorsal ruffling”). This phenomenon depended on FA and actin polymerization but is insensitive to inhibition of actomyosin contractility. While the cell edge protruded extensively, the average FA size decreased, yet the total traction force increased. If FA anchors cell edge protrusion, then why does it decrease in size? And why does the FA traction increase?

Our intuition—backed up by the phase diagram study of our model—is that the viscosity response must entail the following two features (11). First, the membrane tension must decrease to let go of the cell edge; in this way, the cell edge protrusion is upstream of the FA anchorage effect. Second, the dynamical pace of FA assembly/disassembly must increase to generate more nascent FA complexes per unit time, powering a higher total traction force and a faster migration. One consequence of these two features is that the actin retrograde flux should decrease significantly, rendering a more limited FA centripetal growth.

Guided by this intuitive picture, we used an array of high-resolution live-cell imaging techniques to test the model predictions (11). We measured the membrane tension from the recoiling rate of the cortical wound generated by laser ablation and showed that, indeed, the membrane tension decreased upon viscosity increase. Moreover, combining TIRFM and TGT approaches we confirmed that FA sped up its life cycle and more nascent FA complexes were present when the adherent cells were exposed to high viscosity. Finally, the RICM and confocal microscopy data demonstrated that the actin retrograde flux diminished in response to elevated viscosity. These results suggest that, when the cell edge is relaxed upon high viscosity, more polymerization of branching actin network will keep up with the cell protrusion, leading to the decreases in actin retrograde flux and FA size.

Together, by intimately connecting single-molecule approaches and high-resolution experiments with theoretical models, our work collectively supports the notion that FA life cycle and cell edge dynamics modulate each other via the actin cytoskeletons engaged, forming tripartite feedback. Our tripartite feedback model precipitates many deeper questions. For instance, are there biochemical/signaling pathways with diffusible elements that directly link the dynamics of FA and actin cytoskeleton to cell edge? Serving as a signaling hub, how does the dynamics of an FA control its local membrane tension, dorsal ruffling, and polymerization of branching actin network? These pressing questions beg better single-molecule techniques and microscopies and more meaningful theoretical models. From the experimental side, single-molecule tension sensors may also be improved. TGTs are not passive tension sensors as they rupture at high forces, abruptly terminating a cell-matrix conversation. Tension sensors that report on forces

through reversible tension-induced conformational changes (29) or through irreversible rupture while keeping the integrin-substrate engagement may be adopted (30). Moreover, single-molecule tension sensors that report on two or more tension values, ideally over a wide range of forces, would shed light on the entire developmental process of FA (30). From the modeling side, extending the model to the whole-cell scale may help us understand how the collective behaviors of the FA ensemble, cell edge, and cell body determine the cell motility.

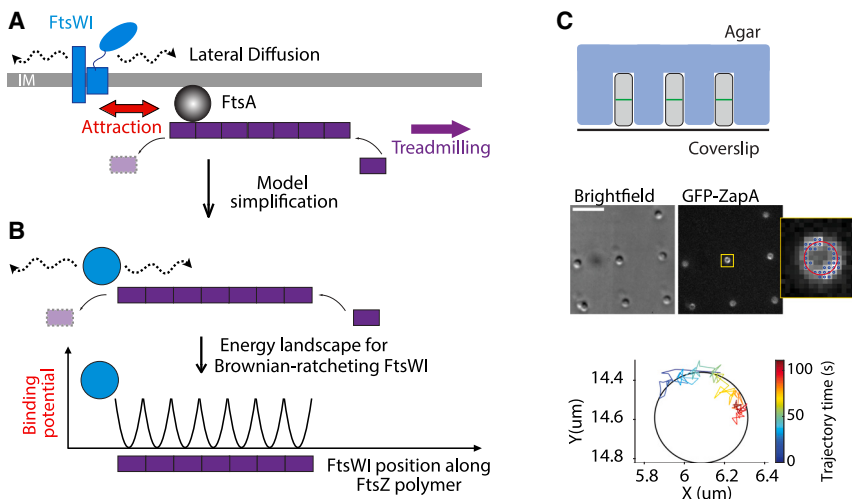
FtsZ-MEDIATED BROWNIAN RATCHETING IN BACTERIAL CELL WALL REMODELING

Bacterial cells have to manage the large turgor pressure to prevent osmotic lysis during cell division, and have to coordinate septal cell wall constriction with the synthesis of new septal peptidoglycan (sPG) at the division plane (31). FtsZ, the bacterial homolog of tubulin GTPase, is the central organizer of cell division for most bacteria (32–34). FtsZ polymerizes at the cytoplasmic face of the inner membrane at midcell to form a ring-like structure (Z-ring). The Z-ring recruits more than a dozen sPG remodeling enzymes and regulators, forming a “divisome,” which initiate septal cell wall constriction (32–34). Single-molecule tracking (SMT) and superresolution live-cell imaging showed that the FtsZ filaments exhibit treadmilling dynamics in which FtsZ polymerizes continuously at one end and depolymerizes at the other end, while all FtsZ monomers remain stationary along the length of the filament (35,36). The treadmilling dynamics drive processive movements of the sPG synthesis enzymes (35,36). How does FtsZ’s treadmilling dynamics with stationary monomers in the cytoplasm drive the persistent and directional movement of cell wall synthesis enzymes in the periplasm? Furthermore, the cell wall constriction rate depended on FtsZ’s treadmilling speed in *B. subtilis* (36) but not in *E. coli* or *S. aureus* (35,37). Given its well-conserved role as the central organizer of cell division, how and why does FtsZ’s treadmilling modulate sPG synthesis activity distinctly in different bacteria?

... Nature almost surely operates by combining chance with necessity, randomness with determinism ...

—Eric Chaisson

Directed and persistent movements require energy inputs. Although FtsZ itself is a GTPase, its rate is 100 times smaller than the FtsZ treadmilling rate (38), suggesting that GTP hydrolysis is not powering the movement. Instead, we asked, can FtsZ treadmilling act as a Brownian ratchet, in which thermal energy is rectified and drives the directed motility of the sPG synthases (Fig. 2, A and B)? That is, FtsZ treadmilling introduces an asymmetry to bias the random diffusion of sPG synthases in the periplasm, upon which the sPG synthase persistently follows the shrinking end of



a treadmilling FtsZ filament. If so, then the real question is: With the realistic parameters, can this Brownian ratchet mechanism quantitatively explain the observed directed motility?

To test this idea, we first exploited an agent-based stochastic modeling approach (39). As a starting point, the model describes the movement of a free sPG synthase as quasi-1D Langevin dynamics (Fig. 2 B): a sPG synthase can freely diffuse along the inner membrane or interact via a binding potential with a treadmilling FtsZ polymer underneath. Importantly, with the model parameters constrained by experimentally measured values, the model can quantitatively explain the observed directed motility and lead to the following picture (39). As the FtsZ subunit at the shrinking end of the polymer falls off, the once-associated sPG synthase is now free to diffuse. However, the next FtsZ subunit in the row presents the binding potential just a short distance away; by chance, the sPG synthase molecule diffuses closer to the new end subunit and is trapped again. With the subsequent FtsZ subunits falling off one after the other, the sPG synthase ratchets forward and persistently tracks the shrinking end of the treadmilling FtsZ polymer, resulting in the directional movement of the sPG synthase that couples its speed to FtsZ's treadmilling speed.

A prediction of this model is that the time duration of sPG synthase's persistent run decreases with increasing treadmilling speed, because the faster FtsZ filament shrinks, the harder for the dissociated sPG synthase to catch up and hence stay at the shrinking end. In contrast, the distance covered by the persistent run is predicted to be biphasic. It reaches the maximum at the FtsZ treadmilling speed of $\sim 30\text{--}40\text{ nm/s}$ and decreases sharply when the treadmilling is too fast for catching up.

In the original SMT setup (35), the molecular trajectories along the septum perimeter were monitored in the TIRFM field, which restricts the observation region to $\sim 200\text{ nm}$ from the coverslip surface. Given that the septum in

FIGURE 2 FtsZ treadmilling-mediated Brownian ratcheting drives directional movements of bacterial septal cell wall remodeling enzymes. (A) Schematized interactions between a FtsZ polymer and sPG synthesis enzymes (e.g., FtsWI). (B) Model formulation of Brownian ratchet mechanism. (C) Microhole experimental setup enables unbiased single-molecule tracking of the sPG synthesis's movement along the perimeter of the septum. Upper: schematics of microhole experiment. The gray rods represent the *E. coli* cells trapped inside the hole and the green line marks the septum of that cell at the initial stage, which is $\sim 1\text{ }\mu\text{m}$ in diameter. Middle: end-on view of the septum. Scale bar, $5\text{ }\mu\text{m}$ (bright field). Lower: typical trajectory of single-molecule tracking of FtsWI along the perimeter of the septum.

E. coli is $\sim 1\text{ }\mu\text{m}$ in diameter, only about an $\sim 600\text{ nm}$ segment of septum perimeter can be visualized. Since the maximum run length is predicted to be $>1000\text{ nm}$, the SMT measurements in a TIRFM field will greatly bias toward the shorter run length. We therefore resorted to the microhole setup (39) (Fig. 2 C), which traps and aligns the *E. coli* in the cylindrical-shaped hole, allowing an end-on view of the septum and hence the unrestricted SMT along the circumference of the septum. With this experimental design, we were able to quantitatively verify the predicted dependences of run duration and length on FtsZ treadmilling speeds, further supporting the Brownian ratchet mechanism (39).

The intuitive mind is a sacred gift and the rational mind is a faithful servant.

—Albert Einstein

What is the role of FtsZ treadmilling in sPG synthesis? And why does the sPG synthesis rate depend on FtsZ treadmilling speed distinctly in different bacteria? The processivity of persistent runs in our Brownian ratchet model hinges on three key parameters, 1) the binding potential between sPG synthase and FtsZ, 2) sPG synthase's diffusion coefficient, and 3) FtsZ treadmilling speed. By controlling sPG synthase diffusion and binding potential, different bacteria may harness the same FtsZ treadmilling machinery to achieve distinct processivities of sPG enzymes.

While the above intuitive picture is exciting, we must be cautious, because it is inferred by our simplistic 1D model. The model needs to be extended to the more realistic 2D to capture the essential geometry of septum and Z-ring (40). Furthermore, the sPG synthase is not a single preexisting protein; instead, it consists of approximately a dozen essential divisome proteins that assemble at the septum *de novo*. How do these proteins find each other and form the sPG synthase complex when they are needed at the septum? What, if

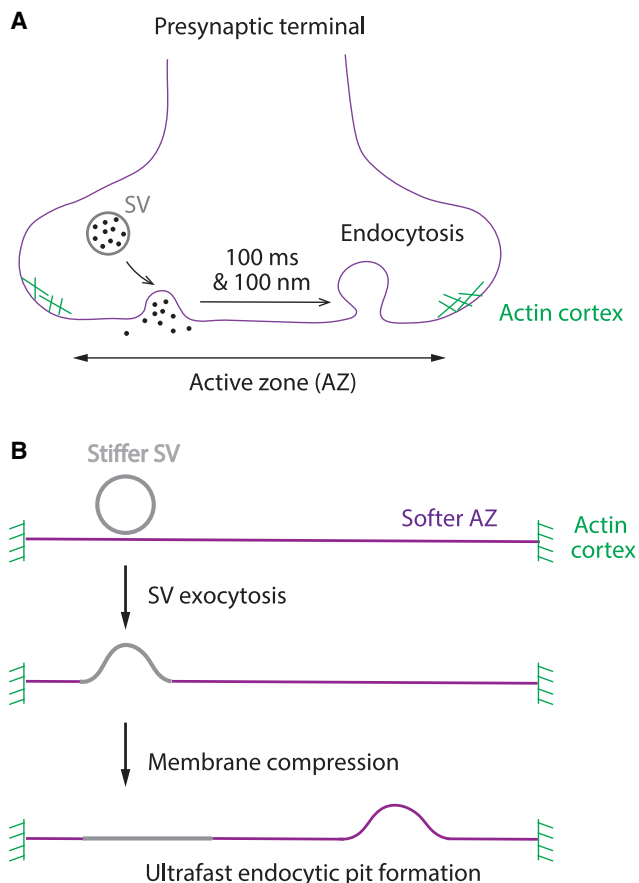


FIGURE 3 Membrane compression from the flattening out of postfusion synaptic vesicles (SVs) drives ultrafast formation of endocytic pit at active zone (AZ). (A) Schematics of experimental characterization of ultrafast coupling between SV exocytosis and endocytosis. (B) Model formulation of membrane compression effects that drives ultrafast endocytic pit formation. Hereby, SV membrane is assumed to be much stiffer than the AZ membrane and the total membrane area is conserved by the actin cortex encircling the AZ.

any, is the role of FtsZ's treadmilling dynamics in synthase assembly? Furthermore, as cell division progresses and FtsZ polymers disassemble, what maintains the spatiotemporal organization of sPG synthesis? Addressing these questions starting from the framework of Brownian ratchet dynamics will be the exciting future directions. In a broader scope, given the lack of linear stepping motors in bacteria, Brownian ratcheting may define a general framework that underlies the directional transport of cargos, shaped by evolution to meet the needs of different cellular milieus. For instance, Brownian ratchet mechanism also drives ParA-mediated bacterial genome partitioning (2,41–43) and the McdA-mediated carboxysome positioning (44).

ULTRAFAST EXOENDOCYTOSIS COUPLING OF SYNAPTIC VESICLES IN NEURONS

Neurons communicate with one another at synapses. When an electrical signal termed “action potential” (AP) travels

along a neuron, it triggers the fusion of synaptic vesicles (SVs) with the plasma membrane at the presynaptic terminal, termed the “active zone” (AZ). Such SV exocytosis releases the neurotransmitters for neuron-neuron communications. This synaptic transmission is extremely fast: up to 500 SVs can be consumed per second per neuron (45,46). Thus, to sustain synaptic transmission the neuron must retrieve the exocytosed SV membrane and proteins rapidly to clear up the SV release sites on the AZ (47), and to replenish the neurotransmitter-filled SVs (48–50). The discovery of ultrafast endocytosis that quickly follows SV exocytosis on the AZ (51–54) may provide an explanation for a remarkable coupling between SV exocytosis and endocytosis. Using the “Zap and Freeze” method that triggers single APs by electrical stimulation, followed by high-pressure freezing to preserve the membrane structure at defined time points, electron micrographs showed that SV exocytosis triggers the ultrafast endocytosis, within ~100 ms and ~100 nm away from the SV fusion sites (Fig. 3 A). Interestingly, this ultrafast endocytosis depends on the similar endocytic machinery for conventional endocytosis in yeast and other mammalian cells (52–55). What drives the 100 ms timescales of endocytosis in neurons when highly similar endocytic machineries in yeast and other mammalian cells completes endocytosis at tens of seconds timescales?

To better appreciate the significance of this mystery, let us summarize the physical mechanisms of endocytosis and the determinants of its timescale. We established that curvature sensing-mediated feedback serves as the central theme to orchestrate the robust spatial-temporal order in endocytosis (56). In brief, many of the endocytic proteins are curvature sensitive. When the local membrane shape is close to the shape preferred by a curvature-sensitive protein, it will promote more recruitment of such proteins (curvature sensing); conversely, binding of curvature-sensitive proteins will deform the membrane to their preferred shape (curvature induction). Curvature sensing and induction therefore form positive feedback. Given the different curvature sensitivities of endocytic proteins, this curvature-mediated feedback can quantitatively capture the observed sequential recruitments of endocytic proteins onto distinct locations of endocytic site. This process tightly couples to the drastic membrane shape changes, leading to a robust endocytic vesicle scission event in both yeast and mammalian cells. The key notion of the model has been supported by many experiments (e.g., (57,58)). In this model, the timescale of endocytosis depends on two processes, i.e., how fast the endocytic proteins get recruited onto the membrane and how fast the membrane changes its shape. Given the typical intracellular concentrations of endocytic proteins and dynamical pace of membrane shape changes, the endocytic timescale is predicted to be ~10–100 s, which are consistent with the experimental measurements across different cell lines.

Now let us rephrase our question. How can neurons achieve ~100–1000 times faster endocytosis while using

the similar collection of endocytic proteins? One way to speed up endocytosis is to increase the local concentrations of endocytic proteins. Indeed, an endocytic protein called dynamin constitutively forms the high-density droplets at the edge of the AZ (59). As dynamin is a well-known “pinchase” for vesicle scission and its knockdown disrupts the ultrafast endocytosis, dynamin droplet formation may enable ultrafast endocytosis through local protein enrichment (59). However, it still needs to be explained how the location and timing of the ultrafast endocytosis tightly couple to the SV exocytosis. While dynamin knockdown dispersed the dynamin droplet and slowed down endocytosis 100-fold, the endocytic membrane pits still emerged as rapidly as in the wild-type (59). This finding suggests that, upon SV fusion, the endocytic membrane pits emerge first, and then invoke the curvature-mediated feedback with the endocytic proteins, leading to vesicle scission. Therefore, the real question becomes: How does SV exocytosis drive the ultrafast formation of endocytic pits?

An idea is salvation by imagination

—Frank Lloyd Wright

In our physics-based model of exoendocytosis coupling (Fig. 3 B) (60), the ultrafast pace of endocytic pit formation stems from the mechanics of SV exocytosis. As the SV membrane flattens out, it compresses the rest of the membrane in the AZ into the endocytic pits. For this model to work, first, it must be energetically favorable for the postfusion SVs to flatten out while some part of the AZ membrane deforms into endocytic pits. The SV is highly enriched in cholesterol and more than 40% of surface area is covered with membrane proteins (61), both of which are well known to rigidify the membrane. Therefore, the SV membrane is probably stiffer than the AZ membrane, thus providing the needed energetic incentive for endocytic pit formation with the SV flattening out. Second, the total membrane area should be conserved; otherwise, SV flattening out will drive the lipids out of the AZ without causing membrane buckling. This was a key model assumption without experimental support at that time.

The model treats the membrane as an elastic sheet and its mechanical energy function contains contributions from bending energy and osmotic pressure. Membrane tension is treated as the Lagrange multiplier that imposes the conservation of the total membrane area. The model simulations start with postfusion SVs that have much larger bending moduli than the AZ membrane and nearly halfway flattened out. With the experimentally measured dimensions of the SV and the AZ in mouse hippocampal synapses and realistic parameters of membrane mechanics, the model can readily recapitulate the observed spatial-temporal pattern of ultrafast endocytic pit formation coupled to SV exocytosis. Therefore, it is physically possible that the membrane compression from SV exocytosis drives the

endocytic pit formation within 50 ms and at the edge of the AZ.

Details make perfection, and perfection is not a detail.

—Leonardo Da Vinci

To experimentally test the key assumption of membrane area conservation, we must know the molecular determinant of the membrane area conservation. Superresolution imaging showed that F-actin forms a dense ring-like structure encircling the AZ (Fig. 3 A) (60). We therefore reasoned that, due to its binding affinity with lipids, F-actin may conserve the total membrane area by acting as a barrier that prevents the lipids from flowing out of the AZ. If so, then disrupting F-actin at the AZ periphery is predicted to inhibit the ultrafast endocytosis; in contrast, preserving F-actin structure by freezing the dynamical exchange of actin monomers is expected to preserve the ultrafast endocytosis. Our Zap and Freeze EM experiment showed that, indeed, ultrafast endocytosis was completely blocked by the latrunculin A treatment that disassembles F-actin, whereas it still occurred in these neurons treated with jasplakinolide, which froze the F-actin structures (60). These findings suggest that, unlike the conventional endocytosis, the presence, rather than the dynamics, of the actin cortex underlies ultrafast endocytosis.

Moving forward, with this central framework we can start to address more in-depth mechanistic questions of exoendocytosis coupling. For instance, changing external parameters (e.g., increasing AP frequency and decreasing temperature from $\sim 35^{\circ}\text{C}$ to room temperature [$\sim 20^{\circ}\text{C}$]) can slow down the endocytic timescale at presynaptic terminal in neurons from 100 ms to 100 s (52). What are the organizational principles that enable such differentiations of endocytosis machinery? Related, with high-frequency AP stimulations (e.g., > 10 Hz), the endocytosis of SV may not complete in between AP stimulations. If so, then how will the stranded SV membrane and proteins impact the AZ geometry, the endocytosis, and the subsequent SV exocytosis? Moreover, the model implies that ultrafast endocytosis critically depends on the quantitative difference in the membrane bending moduli between SV and AZ. Can we directly measure the membrane bending moduli of SV and AZ at presynaptic terminal in neurons?

CONCLUSION AND PERSPECTIVES

We have to remember that what we observe is not nature herself, but nature exposed to our method of questioning.

—Werner Carl Heisenberg

Single-molecule and superresolution microscopies revolutionize cell biology by revealing the fascinating details, which help formulate the right questions, put strong constraints on the possible physical mechanisms, and greatly facilitate the

development of theoretical models. While rooted in fundamental physical laws, the art of theoretical models should follow the simplest possible spirit that is driven by the intuitive synthesis of existing data and interfaces with experimental testing. As discussed above, organically integrating single-molecule and superresolution microscopies with this style of theoretical models provides an exciting approach, which helps deepen our understanding of cellular processes, opens more fronts of cell biology research, and ultimately, pushes the limits of both experiment and theory.

ACKNOWLEDGMENTS

This work was supported by start-up funds from the Johns Hopkins University School of Medicine, Johns Hopkins Catalyst award, the National Science Foundation (2105837 and 2148534), and the NIH (1RO1 GM148459-01) to J.L. The funders had no role in study design, data collection and analysis, decision to publish, or preparation of the manuscript. T.H. is an investigator of the Howard Hughes Medical Institute.

AUTHOR CONTRIBUTIONS

J.L. and T.J.H. conceived, designed, wrote, reviewed, and edited the manuscript.

DECLARATION OF INTERESTS

T.H. is an immediate family member of one of the members of the Biophysical Journal Editorial Board.

REFERENCES

1. Mora, T., and W. Bialek. 2011. Are Biological Systems Poised at Criticality? *J. Stat. Phys.* 144:268–302.
2. Hu, L., J. Rech, ..., J. Liu. 2021. Spatial control over near-critical-point operation ensures fidelity of ParABS-mediated DNA partition. *Biophys. J.* 120:3911–3924.
3. Bershadsky, A. D., N. Q. Balaban, and B. Geiger. 2003. Adhesion-Dependent Cell Mechanosensitivity. *Annu. Rev. Cell Dev. Biol.* 19:677–695.
4. Gardel, M. L., I. C. Schneider, ..., C. M. Waterman. 2010. Mechanical integration of actin and adhesion dynamics in cell migration. *Annu. Rev. Cell Dev. Biol.* 26:315–333.
5. Ribeiro-Silva, J. C., A. A. Miyakawa, and J. E. Krieger. 2021. Focal adhesion signaling: vascular smooth muscle cell contractility beyond calcium mechanisms. *Clin. Sci.* 135:1189–1207.
6. Paszek, M. J., N. Zahir, ..., V. M. Weaver. 2005. Tensional homeostasis and the malignant phenotype. *Cancer Cell.* 8:241–254.
7. Wu, Z., S. V. Plotnikov, ..., J. Liu. 2017. Two Distinct Actin Networks Mediate Traction Oscillations to Confer Focal Adhesion Mechanosensing. *Biophys. J.* 112:780–794.
8. Plotnikov, S. V., A. M. Pasapera, ..., C. M. Waterman. 2012. Force Fluctuations within Focal Adhesions Mediate ECM-Rigidity Sensing to Guide Directed Cell Migration. *Cell.* 151:1513–1527.
9. Geiger, B., J. P. Spatz, and A. D. Bershadsky. 2009. Environmental sensing through focal adhesions. *Nat. Rev. Mol. Cell Biol.* 10:21–33.
10. Jo, M. H., B. C. Kim, ..., T. Ha. 2021. Molecular Nanomechanical Mapping of Histamine-Induced Smooth Muscle Cell Contraction and Shortening. *ACS Nano.* 15:11585–11596.
11. Pittman, M., E. Iu, ..., Y. Chen. 2022. Membrane Ruffling is a Mechanosensor of Extracellular Fluid Viscosity. *Nat. Phys.* 18:1112–1121.
12. Tao, J., and S. X. Sun. 2015. Active Biochemical Regulation of Cell Volume and a Simple Model of Cell Tension Response. *Biophys. J.* 109:1541–1550.
13. Reichl, E. M., Y. Ren, ..., D. N. Robinson. 2008. Interactions between myosin and actin crosslinkers control cytokinesis contractility dynamics and mechanics. *Curr. Biol.* 18:471–480.
14. Zaidel-Bar, R., R. Milo, ..., B. Geiger. 2007. A paxillin tyrosine phosphorylation switch regulates the assembly and form of cell-matrix adhesions. *J. Cell Sci.* 120:137–148.
15. Grashoff, C., B. D. Hoffman, ..., M. A. Schwartz. 2010. Measuring mechanical tension across vinculin reveals regulation of focal adhesion dynamics. *Nature.* 466:263–266.
16. Hu, K., L. Ji, ..., C. M. Waterman-Storer. 2007. Differential transmission of actin motion within focal adhesions. *Science.* 315:111–115.
17. Alexandrova, A. Y., K. Arnold, ..., A. B. Verkhovsky. 2008. Comparative Dynamics of Retrograde Actin Flow and Focal Adhesions: Formation of Nascent Adhesions Triggers Transition from Fast to Slow Flow. *PLoS One.* 3:e3234.
18. Chugh, P., and E. K. Paluch. 2018. The actin cortex at a glance. *J. Cell Sci.* 131:jcs186254.
19. Hirata, H., H. Tatsumi, ..., M. Sokabe. 2014. Force-dependent vinculin binding to talin in live cells: a crucial step in anchoring the actin cytoskeleton to focal adhesions. *Am. J. Physiol. Cell Physiol.* 306:C607–C620.
20. Walcott, S., and S. X. Sun. 2010. A mechanical model of actin stress fiber formation and substrate elasticity sensing in adherent cells. *Proc. Natl. Acad. Sci. USA.* 107:7757–7762.
21. Li, J., and T. A. Springer. 2017. Integrin extension enables ultrasensitive regulation by cytoskeletal force. *Proc. Natl. Acad. Sci. USA.* 114:4685–4690.
22. del Rio, A., R. Perez-Jimenez, ..., M. P. Sheetz. 2009. Stretching Single Talin Rod Molecules Activates Vinculin Binding. *Science.* 323:638–641.
23. Kong, F., A. J. García, ..., C. Zhu. 2009. Demonstration of catch bonds between an integrin and its ligand. *JCB (J. Cell Biol.).* 185:1275–1284.
24. Chan, C. E., and D. J. Odde. 2008. Traction Dynamics of Filopodia on Compliant Substrates. *Science.* 322:1687–1691.
25. Kanchanawong, P., G. Shtengel, ..., C. M. Waterman. 2010. Nanoscale architecture of integrin-based cell adhesions. *Nature.* 468:580–584.
26. Wang, X., and T. Ha. 2013. Defining Single Molecular Forces Required to Activate Integrin and Notch Signaling. *Science.* 340:991–994.
27. Wang, X., J. Sun, ..., T. Ha. 2015. Integrin Molecular Tension within Motile Focal Adhesions. *Biophys. J.* 109:2259–2267.
28. Jo, M. H., W. T. Cottle, and T. Ha. 2019. Real-Time Measurement of Molecular Tension during Cell Adhesion and Migration Using Multiplexed Differential Analysis of Tension Gauge Tethers. *ACS Biomater. Sci. Eng.* 5:3856–3863.
29. Li, H., C. Zhang, ..., Z. Liu. 2021. A reversible shearing DNA probe for visualizing mechanically strong receptors in living cells. *Nat. Cell Biol.* 23:642–651.
30. Jo, M. H., P. Meneses, ..., T. Ha. 2024. Determination of single-molecule loading rate during mechanotransduction in cell adhesion. *Science.* 383:1374–1379.
31. Egan, A. J. F., J. Errington, and W. Vollmer. 2020. Regulation of peptidoglycan synthesis and remodelling. *Nat. Rev. Microbiol.* 18:446–460.
32. McQuillen, R., and J. Xiao. 2020. Insights into the Structure, Function, and Dynamics of the Bacterial Cytokinetic FtsZ-Ring. *Annu. Rev. Biophys.* 49:309–341.
33. Cameron, T. A., and W. Margolin. 2024. Insights into the assembly and regulation of the bacterial divisome. *Nat. Rev. Microbiol.* 22:33–45.
34. Du, S., and J. Lutkenhaus. 2017. Assembly and activation of the *Escherichia coli* divisome. *Mol. Microbiol.* 105:177–187.

35. Yang, X., Z. Lyu, ..., J. Xiao. 2017. GTPase activity–coupled treadmilling of the bacterial tubulin FtsZ organizes septal cell wall synthesis. *Science*. 355:744–747.

36. Bisson-Filho, A. W., Y.-P. Hsu, ..., E. C. Garner. 2017. Treadmilling by FtsZ filaments drives peptidoglycan synthesis and bacterial cell division. *Science*. 355:739–743.

37. Monteiro, J. M., A. R. Pereira, ..., M. G. Pinho. 2018. Peptidoglycan synthesis drives an FtsZ-treadmilling-independent step of cytokinesis. *Nature*. 554:528–532.

38. de Boer, P., R. Crossley, and L. Rothfield. 1992. The essential bacterial cell-division protein FtsZ is a GTPase. *Nature*. 359:254–256.

39. McCausland, J. W., X. Yang, ..., J. Liu. 2021. Treadmilling FtsZ polymers drive the directional movement of sPG-synthesis enzymes via a Brownian ratchet mechanism. *Nat. Commun.* 12:609.

40. Hu, L., A. Perez, ..., J. Liu. 2024. FtsZ-mediated spatial-temporal control over septal cell wall synthesis. Preprint at bioRxiv. <https://doi.org/10.1101/2024.2001.2029.577872>.

41. Hu, L., A. G. Vecchiarelli, ..., J. Liu. 2015. Directed and persistent movement arises from mechanochemistry of the ParA/ParB system. *Proc. Natl. Acad. Sci. USA*. 112:E7055–E7064.

42. Hu, L., A. G. Vecchiarelli, ..., J. Liu. 2017. Brownian Ratchet Mechanism for Faithful Segregation of Low-Copy-Number Plasmids. *Biophys. J.* 112:1489–1502.

43. Le Gall, A., D. I. Cattoni, ..., M. Nollmann. 2016. Bacterial partition complexes segregate within the volume of the nucleoid. *Nat. Commun.* 7:12107.

44. MacCready, J. S., P. Hakim, ..., D. C. Ducat. 2018. Protein gradients on the nucleoid position the carbon-fixing organelles of cyanobacteria. *Elife*. 7:e39723.

45. Kopp-Scheinflug, C., S. Tolnai, ..., R. Rübsamen. 2008. The medial nucleus of the trapezoid body: Comparative physiology. *Neuroscience*. 154:160–170.

46. Lorteije, J. A. M., S. I. Rusu, ..., J. G. G. Borst. 2009. Reliability and Precision of the Mouse Calyx of Held Synapse. *J. Neurosci.* 29:13770–13784.

47. Neher, E. 2010. What is Rate-Limiting during Sustained Synaptic Activity: Vesicle Supply or the Availability of Release Sites. *Front. Synaptic Neurosci.* 2:144.

48. Kononenko, N. L., and V. Hauke. 2015. Molecular mechanisms of presynaptic membrane retrieval and synaptic vesicle reformation. *Neuron*. 85:484–496.

49. Chanaday, N. L., M. A. Cousin, ..., J. R. Morgan. 2019. The Synaptic Vesicle Cycle Revisited: New Insights into the Modes and Mechanisms. *J. Neurosci.* 39:8209–8216.

50. Saheki, Y., and P. De Camilli. 2012. Synaptic vesicle endocytosis. *Cold Spring Harbor Perspect. Biol.* 4:a005645.

51. Sun, J.-Y., X.-S. Wu, and L.-G. Wu. 2002. Single and multiple vesicle fusion induce different rates of endocytosis at a central synapse. *Nature*. 417:555–559.

52. Watanabe, S., B. R. Rost, ..., E. M. Jorgensen. 2013. Ultrafast endocytosis at mouse hippocampal synapses. *Nature*. 504:242–247.

53. Watanabe, S., T. Trimbuch, ..., E. M. Jorgensen. 2014. Clathrin regenerates synaptic vesicles from endosomes. *Nature*. 515:228–233.

54. Watanabe, S., Q. Liu, ..., E. M. Jorgensen. 2013. Ultrafast endocytosis at Caenorhabditis elegans neuromuscular junctions. *Elife*. 2:e00723.

55. Watanabe, S., L. E. Mamer, ..., E. M. Jorgensen. 2018. Synaptotagmin and Endophilin Mediate Neck Formation during Ultrafast Endocytosis. *Neuron*. 98:1184–1197.e6.

56. Liu, J., Y. Sun, ..., G. F. Oster. 2009. The Mechanochemistry of Endocytosis. *PLoS Biol.* 7:e1000204.

57. Cail, R. C., C. R. Shirazinejad, and D. G. Drubin. 2022. Induced nanoscale membrane curvature bypasses the essential endocytic function of clathrin. *J. Cell Biol.* 221:e202109013.

58. Zhao, W., L. Hanson, ..., B. Cui. 2017. Nanoscale manipulation of membrane curvature for probing endocytosis in live cells. *Nat. Nanotechnol.* 12:750–756.

59. Imoto, Y., S. Raychaudhuri, ..., S. Watanabe. 2022. Dynamin is primed at endocytic sites for ultrafast endocytosis. *Neuron*. 110:2815–2835.e13.

60. Ogunmowo, T. H., H. Jing, ..., J. Liu. 2023. Membrane compression by synaptic vesicle exocytosis triggers ultrafast endocytosis. *Nat. Commun.* 14:2888.

61. Takamori, S., M. Holt, ..., R. Jahn. 2006. Molecular anatomy of a trafficking organelle. *Cell*. 127:831–846.